Journal of Magnetic Resonance 299 (2019) 188–195

Contents lists available at ScienceDirect

Journal of Magnetic Resonance

journal homepage: www.elsevier.com/locate/jmr

Hyperpolarized [^{15}N]nitrate as a potential long lived hyperpolarized contrast agent for MRI

Ayelet Gamliel, Sivaranjan Uppala, Gal Sapir, Talia Harris, Atara Nardi-Schreiber, David Shaul, Jacob Sosna, J. Moshe Gomori, Rachel Katz-Brull *

Department of Radiology, Hadassah Medical Center, Hebrew University of Jerusalem, The Faculty of Medicine, Jerusalem, Israel

ARTICLE INFO

Article history:
Received 22 November 2018
Revised 31 December 2018
Accepted 3 January 2019
Available online 4 January 2019

Keywords:
T_1 relaxation
Dissolution-dynamic nuclear polarization
Nitrate and nitrite ions
Contrast
Tissue retention

ABSTRACT

Reports on gadolinium deposits in the body and brains of adults and children who underwent contrast-enhanced MRI examinations warrant development of new, metal free, contrast agents for MRI. Nitrate is an abundant ion in mammalian biochemistry and sodium nitrate can be safely injected intravenously. We show that hyperpolarized [^{15}N]nitrate can potentially be used as an MR tracer. The ^{15}N site of hyperpolarized [^{15}N]nitrate showed a T_1 of more than 100 s in aqueous solutions, which was prolonged to more than 170 s below 20 °C. Capitalizing on this effect for polarization storage we obtained a visibility window of 9 min in blood. Conversion to [^{15}N]nitrite, the bioactive reduced form of nitrate, was not observed in human blood and human saliva in this time frame. Thus, [^{15}N]nitrate may serve as a long-lived hyperpolarized tracer for MR. Due to its ionic nature, the immediate applications appear to be perfusion and tissue retention imaging.

1. Introduction

New MRI contrast agents are needed as long lasting gadolinium deposits have been observed in people who have undergone a contrast-enhanced MRI examination [1–9] and with the rise of this metal in the environment, which is linked to medical use [10]. Gadolinium deposits in humans have not yet been associated with adverse events, excluding the nephrogenic systemic fibrosis disease which had been effectively almost eradicated with screening of patients for renal function prior to contrast administration [10,11]. Also, some gadolinium chelates appear to be much safer than others – meaning that the gadolinium ion is hardly released in the body [12,13]. Nevertheless, new, metal-free, and safe contrast agents for MRI, that leave no traces behind, are needed. Given the high number of such examinations – about 30 million annually worldwide [14], research and development in this direction are warranted.

The inorganic nitrate anion (NO_3^-) is found in many foods, especially vegetables [15], and is an endogenous mammalian metabolite. NO_3^- in the plasma is both the result of nitrate from the diet and the final product of nitric oxide (NO) metabolism [16–18]. The biological activities of nitrate originate from the reduction to nitrite [19,20] which in turn is reduced to the vasodilator NO. The reduction of nitrate to nitrite in mammals is catalyzed mainly by the bacterial nitrate-reductase enzymes present in saliva [16,19–24], while in mammalian tissues the rate of this reduction is low [23].

Hence, nitrite (NO_2^-) is a bioactive ion in mammals and serves as a reservoir of NO, while nitrate is considered biologically relatively inactive [23] and was even used as a control in studies of nitrite activity [25]. The half-life of nitrate in the circulation is about 5–6 h while that of nitrite is 20 min [16]. About 60–70% of the plasma nitrate is excreted in the urine [15,26] and only about 5% of ingested nitrate is converted to nitrite [15]. In healthy volunteers, a concentrated solution of sodium nitrate (0.15 M, 0.75 L, 1 h) was injected intravenously without any side-effects [27]. Since the discovery that nitrate reductase activity occurs also in mammalian tissues and not only in bacteria [9], much research into the nature and level of this activity ensued [28] and beneficial effects of nitrates have been reported in the context of several diseases and conditions such as diabetes [29] and heart failure [30].

Here we propose a new use for this widely used and researched endogenous metabolite as a hyperpolarized contrast agent for MRI. We show that when labeled with the stable isotope ^{15}N, the signal of nitrate can be enhanced 5,300-fold relative to its thermal signal at 5.8 T corresponding to 1% polarization, and this enhanced signal will decay slowly before injection even in biocompatible saline solutions. This new use relies on the dissolution dynamic nuclear polarization technique (dDNP) which offers 3–4 orders of

* Corresponding author.
E-mail address: rkb@hadassah.org.il (R. Katz-Brull).

https://doi.org/10.1016/j.jmr.2019.01.001
1090-7807/

magnitude increase in the signal of small molecules in solution for nuclear magnetic resonance (NMR) detection [31]. As this enhanced signal achieved with dDNP will decay at a rate determined by the longitudinal relaxation time (T_1) of the hyperpolarized site, sites with long T_1s are the holy grail of dDNP studies. Non-protonated carbons have relatively long T_1 and have been used as metabolic and non-metabolic dDNP probes, for example, [1-^{13}C]pyruvate with a T_1 of 65 s [32] and [^{13}C]urea with a T_1 of 58 s [33], respectively. The T_1s of ^{15}N sites have been reported to be similar and longer when the nitrogen is not covalently bound to a hydrogen. For example, pyridine, acetonitrile, and nitrobenzene, showed T_1s of 58 s, 110 s, and 135 s [34], respectively, and quaternary amines such as [^{15}N]choline and [^{15}N]trimethylphenylammonium ([^{15}N]TMPA) showed T_1s of 200 s [35] and 275 s [36], respectively. It was also shown that the T_1 of ^{15}N could be prolonged by deuterium substitution of protons that are remote to the ^{15}N site [35–37] and by substitution of exchangeable protons directly bound to ^{15}N sites [38,39]. This technology has been applied previously for the observation of ^{15}N sites in compounds that are of metabolic potential [35,37,40], and in non-metabolic compounds aimed as contrast agents for perfusion or tissue retention imaging [38]. Additionally, it is well known that temperature will influence a site's T_1. In 1970, Saluvare et al. [41] reported that the T_1 of the ^{15}N site in nitrate varied inversely with the temperature, showing an increase in the T_1 from ≈100 s at 100 °C to ≈300 s at 10 °C. Based on the above prior research we hypothesized that [^{15}N]nitrate could be hyperpolarized and, in this state, serve as a valuable contrast agent with favorable visualization time window and safety profile for intravenous injection, which is the common administration route for contrast material on MRI examinations. Our investigation shows hyperpolarized [^{15}N]nitrate for the first time and discusses routes to maintain the polarization at high levels prior to the injection and the likely signal behavior in the body.

2. Results

2.1. [^{15}N]nitrate is observed in a hyperpolarized state and its decay is not significantly affected by water protonation or salinity

Applying the dDNP technology to formulations of [^{15}N]nitrate with the trityl radical we could observe the hyperpolarized state of [^{15}N]nitrate in solution at 5.8 T, for about 10 min (Fig. 1a). The maximal enhancement factor, calculated for the 1st signal in solution, was 5,300, corresponding to 1% polarization. This enhancement factor was obtained following 2.5 h of polarization at 1.5–1.6 K. This ^{15}N polarization level (1%) compares well with other measurements of ^{15}N in other molecules (3.1–5.3% after 1–3 h at 1.4–1.5 K) [35,37,38,40]. Other enhancement factors that were found on varied experimental conditions are summarized in the Supporting Information S1.

The T_1 of the ^{15}N site in [^{15}N]nitrate was long – reaching 109 ± 9 s (n = 12) in D_2O at a temperature range of 34–44 °C (Fig. 1b). However, for several hyperpolarized compounds, dissolution in D_2O has been shown to prolong the T_1 time significantly [38,42]. For this reason, we were interested in testing whether this long T_1 will remain also in naturally abundant water. We found that the [^{15}N]nitrate T_1 was not significantly affected by the water protonation (Fig. 1b), with the T_1 in water reaching 98 ± 5 s (n = 2). For biological applications, it is necessary to investigate the T_1 in solutions isosmotic to blood plasma (physiological saline, ~300 mOsm), such that they can be safely injected. In general, it has been shown that in such saline solutions the hyperpolarized site's T_1 is shortened [42,43]. Dissolution of hyperpolarized [^{15}N]nitrate in physiological saline did not reduce its T_1, which was found to be 102 ± 5 s (n = 2) (Fig. 1b). These findings suggested that the T_1 relaxation of [^{15}N]nitrate is relatively immune to changes in the basic physicochemical properties of the lattice, and therefore are encouraging with regards to the potential use of [^{15}N]nitrate as a long-lived contrast agent for MRI.

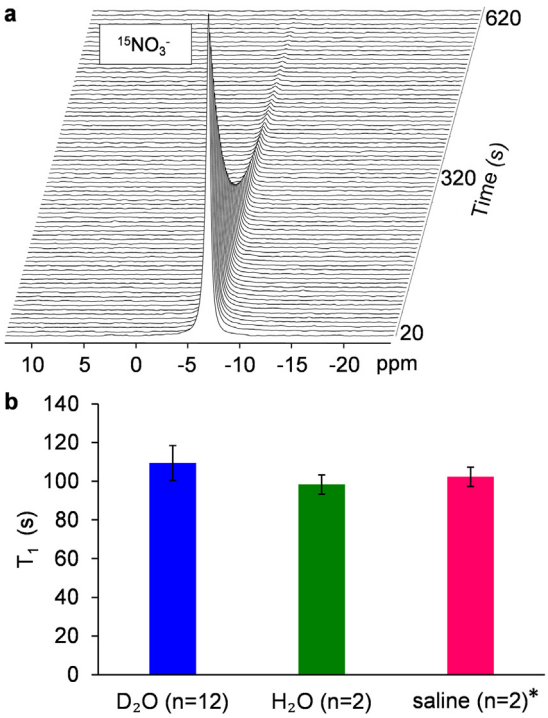

Fig. 1. Observation of hyperpolarized [^{15}N]nitrate and the effects of solvent protonation and salinity on its T_1. (a) Stacked ^{15}N spectra of hyperpolarized sodium [^{15}N]nitrate in D_2O. The spectra were recorded with a flip angle of 10° and a repetition time of 8 s. The time frame of 20–620 s from the onset of the dissolution process is shown. (b) T_1 values of hyperpolarized [^{15}N]nitrate in solution, at concentrations of 19–29 mM sodium [^{15}N]nitrate. T_1s were determined in D_2O, H_2O, and medical grade physiological saline (154 mM NaCl in H_2O), at a temperature range of 34–44 °C. *One sample was dissolved in 4 mL of saline solution and another sample was dissolved in 4 mL of saline which were then mixed with 1 mL human saliva (experiment to be described further in the following). The T_1 values and the exact concentration of sodium [^{15}N]nitrate in individual dissolutions are given in the Supporting Information S1. The temperature in the NMR tube was continuously monitored during the hyperpolarization decay. Because the temperature changed during the hyperpolarized decay, a temperature range is reported (Methods and Supporting Information S5).

2.2. Metabolism of hyperpolarized [^{15}N]nitrate is not seen in body fluids

In order to predict the stability of hyperpolarized [^{15}N]nitrate *in vivo*, we monitored the ^{15}N signal upon dissolution of hyperpolarized [^{15}N]nitrate in human blood and saliva. In order to monitor the potential conversion of [^{15}N]nitrate to [^{15}N]nitrite in these fluids, we first aimed at characterizing the hyperpolarized signal of [^{15}N]nitrite (Fig. 2). The ^{15}N chemical shift of the [^{15}N]nitrite was 226.2 ppm (Fig. 2d), and its T_1 was found to be 14.8 ± 0.6 s (n = 2) and 13.6 ± 0.5 s (n = 2) in D_2O and in H_2O, respectively. The effect of this shorter T_1 of [^{15}N]nitrite compared to [^{15}N]nitrate can be observed in the co-polarization and simultaneous decay experiment shown in Fig. 2a, which demonstrates the smaller and faster decaying signal of hyperpolarized [^{15}N]nitrite, although its concentration was 1.6-fold higher. While the signal of the [^{15}N]nitrate can be observed for more than 500 s, the [^{15}N]nitrite signal is observed for only 55 s (Fig. 2a). We attribute this smaller signal to the fast decay due to T_1, however, we cannot rule out differences in maxi-

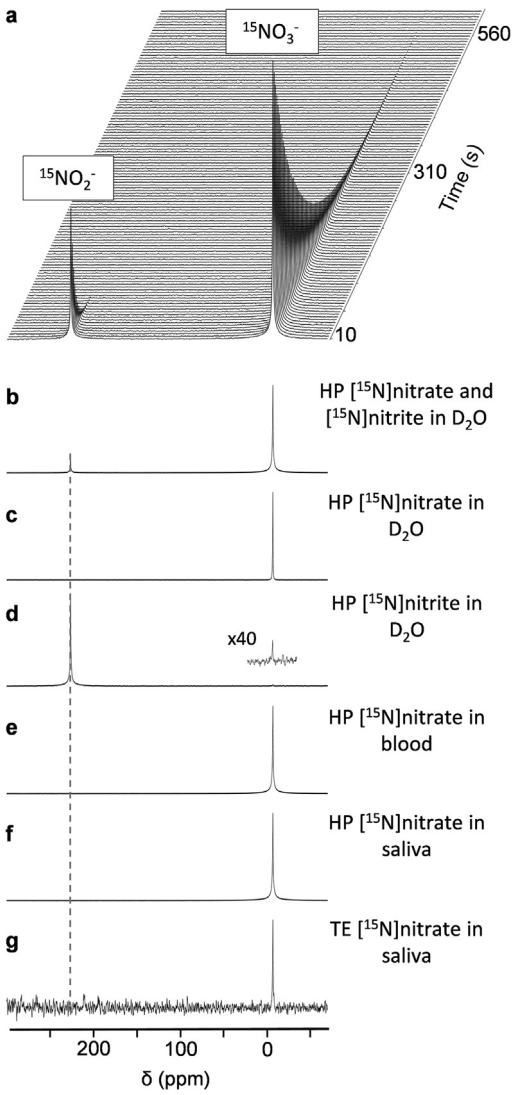

Fig. 2. Hyperpolarized spectra of [^{15}N]nitrate and [^{15}N]nitrite. (a) ^{15}N spectra of co-polarized sodium [^{15}N]nitrate and sodium [^{15}N]nitrite in D_2O (29 mM and 47 mM, respectively), at 37–42 °C. The signals of [^{15}N]nitrate and [^{15}N]nitrite appear at −6.8 and 226.2 ppm, respectively. (b) A summation of the spectra shown in a), in which both of the signals were observed (a total of 15 spectra with repetition time of 5 s, recorded with a flip angle of 10°). (c) A summation of the spectra recorded from a hyperpolarized sample of sodium [^{15}N]nitrate in D_2O (28 mM), at 37–44 °C, (a total of 60 spectra with repetition time of 8 s, recorded with a flip angle of 10°). (d) A summation of the spectra recorded from a hyperpolarized sample of sodium [^{15}N]nitrite in D_2O (37 mM), at 38–41 °C (a total of 15 spectra with a repetition time of 5 s, recorded with a flip angle of 10°). A small hyperpolarized [^{15}N]nitrate signal is observed which may be due to an impurity. (e) A summation of the spectra recorded from a hyperpolarized sample of sodium [^{15}N]nitrate (25 mM) in a blood and saline mixture, at 32–36 °C, (a total of 48 spectra with repetition time of 5 s, recorded with a flip angle of 10°). (f) A summation of the spectra recorded from a hyperpolarized sample of sodium [^{15}N]nitrate (18 mM) in a saliva and saline mixture, at 37–42 °C, (a total of 82 spectra with repetition time of 5 s, recorded with a flip angle of 10°). (g) A summation of thermal equilibrium spectra of sodium [^{15}N]nitrate (18 mM) in a saliva and saline mixture (same sample as in f), recorded at room temperature for 20 h, (a total of 12,000 averages with repetition time of 6 s, recorded with a flip angle of 10°). The spectra are presented with an exponential multiplication of 10 Hz. The line widths of the signals prior to the exponential multiplication were as follows: in (a) and (b) the [^{15}N]nitrate signal 3.2 Hz and the [^{15}N]nitrite signal 3.6 Hz; in (c) 1.1 Hz; in (d) 4.4 Hz; in (e) 4.3 Hz, in (f) 2.1 Hz; and in (g) 1.6 Hz. HP – hyperpolarized; TE – thermal equilibrium.

mal solid-state polarization levels that may have been obtained for the two compounds or differences in the buildup time constants. Nevertheless, although the T_1 of [^{15}N]nitrite is much shorter, it appears sufficiently long that a conversion of [^{15}N]nitrate to [^{15}N]nitrite could be observed during the hyperpolarization decay, (assuming that the reaction itself does not lead to loss of polarization).

In the next step, we wanted to examine the stability of [^{15}N]nitrate in blood – *i.e.* we have searched for signs of conversion to [^{15}N]nitrite. To this end, hyperpolarized [^{15}N]nitrate was dissolved in 4 mL of medical grade saline and quickly injected to an NMR tube containing 10 mL of whole human blood (healthy volunteer), to form a homogenous mixture, and the hyperpolarized signal was monitored for 4 min at 32–36 °C. The T_1 was found to be 29 ± 1 s (the error represents the 95% confidence interval for the individual fit). The final concentration of the [^{15}N]nitrate in this saline/blood mixture was 25 mM. Throughout the decay time, only the [^{15}N]nitrate signal was detected. Also, when averaging all of the spectra that showed a signal, still the nitrate signal was the only signal that could be detected (Fig. 2e). This result suggests that the nitrate stability was not affected by the contact with the blood components. NO_2^- formation, if any, occurred with such a low rate that it was outside the current limits of detection.

Although the intended route of administration for hyperpolarized [^{15}N]nitrate is intravenous, the entero-salivary circulation recycles nitrate from the blood to the saliva, where it can be bacterially converted to [^{15}N]nitrite. For this reason it was important to determine also the potential conversion to hyperpolarized [^{15}N]nitrite in human saliva. To this end, hyperpolarized [^{15}N]nitrate was dissolved in 4 mL of medical grade saline and quickly injected to an NMR tube containing 1 mL of human saliva from a healthy volunteer (not using anti-bacterial mouth wash). The [^{15}N]nitrate hyperpolarized signal was monitored for more than 400 s at a temperature range of 37–42 °C. Throughout this time, only the [^{15}N]nitrate signal was observed and a hyperpolarized [^{15}N]nitrite signal was not observed (Fig. 2f). To test for the presence of [^{15}N]nitrite in this saline-saliva sample after the hyperpolarized state had decayed, the same sample was scanned at thermal equilibrium as well. The sample was scanned for 20 h, at room temperature. The summed spectrum shows the [^{15}N]nitrate signal only (Fig. 2g).

These results suggest that [^{15}N]nitrate was not metabolized in blood or in saliva of the individual volunteer at detectable levels. Further tests with human saliva, conducted for longer measurement times, are described in the Supporting Information S2.

2.3. Hyperpolarized [^{15}N]nitrate exhibits prolonged T_1 in colder solutions

Saluvare et al. [41] have previously shown that the T_1 of nitrate can be prolonged at colder temperatures. For the duration required for transfer of the hyperpolarized solution from the polarizer to the subject, prior to intravenous administration (storage duration), the temperature of the solution is not limited to body temperature. Therefore, it may be beneficial to store the hyperpolarized solution at a colder temperature. To test this possibility, we designed an experimental system in which the hyperpolarized [^{15}N]nitrate solution is either 1) heated and directly injected to the spectrometer or 2) cooled down (with online temperature monitoring), and then injected to an NMR tube in the spectrometer where the temperature is continuously monitored as well, and the T_1 decay is determined in parallel. Hyperpolarized decays in temperatures at a range of 10–50 °C were monitored in this way (Fig. 3). At a range of temperatures close to the human body temperature, 34–44 °C, the T_1 was found to be 109 ± 9 s (n = 12), and at 40–50 °C the T_1 was similar at 105 s (n = 1). Despite many attempts to analyze segments of the decay data and resolve better a possible dependence of the decay rate on temperature, we could not detect any such dependence and we concluded that in the temperature range of 34–50 °C, the T_1 of [^{15}N]nitrate does not change. However, at temperatures of 20–23 °C the T_1 was prolonged, reaching 139 ± 6 s

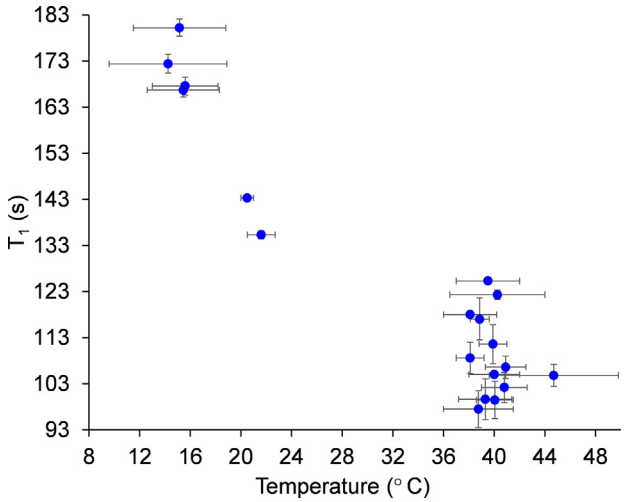

Fig. 3. The dependence of the ^{15}N T_1 of sodium [^{15}N]nitrate on temperature. Solutions of sodium [^{15}N]nitrate at 11–29 mM in D_2O were used. The temperature was monitored online with an MRI compatible temperature sensor. For each point - the X-axis error bar represents the temperature range in which the T_1 was determined, and the Y-axis error bar represents the 95% confidence interval for the individual fit (see Methods). The data points shown here in the range of 34–44 °C are also included in Fig. 1b.

(n = 2), and at 10–19 °C the T_1 was found to be 172 ± 6 s (n = 4). These findings support the possibility that in order to preserve the hyperpolarized state of [^{15}N]nitrate it is advantageous to quickly cool the hyperpolarized solution.

2.4. Storage of hyperpolarized [^{15}N]nitrate in cold solution enables prolonged use for injection

This prolonged T_1 of [^{15}N]nitrate in colder solutions can be capitalized on when observing hyperpolarized [^{15}N]nitrate signal *in vivo*, in particular when multiple perfusion measurements are desired, such that the hyperpolarized solution must be stored for long time periods before injection. To demonstrate the potential advantage of cold storage of the hyperpolarized solution for repeated injections, Fig. 4 demonstrates the visibility of this signal in blood for up to 9 min, while in a previous injection to blood the signal was observed for only 4 min (Fig. 2e, decay not shown). To achieve this dramatic prolongation, the hyperpolarized [^{15}N]nitrate solution was injected to a collection tube placed in an ice-water bath in the fringe field of the magnet and containing 1 mL of ice-cold saline at (2 °C). The hyperpolarized solution reaches the collection tube at a minimum of 26–27 °C and cools down throughout the duration of the experiment. Small amounts of this cold hyperpolarized [^{15}N]nitrate solution (about 1 mL) were then injected into a blood sample (4.5 mL) already placed in the NMR spectrometer and maintained at 36 °C. The small amounts of hyperpolarized solution were added to the blood sample at 0, 3, 6, 7.25, and 9.17 min from arrival of the solution to the collection tube. The corresponding solution temperatures upon injection to the blood sample were 16.4, 5.8, 2.9, 2.1, and 1.7 °C. The signal of hyperpolarized [^{15}N]nitrate was observed in the blood for 2.9, 2.2, 1.0 and 0.6 min for the first four injections (marked 1–4 in Fig. 4a). In the last injection, the signal was observed only in one spectrum (marked 5 in Fig. 4a, signal to noise ratio of 4). This experiment demonstrates the feasibility of storing the polarization of a single hyperpolarized [^{15}N]nitrate dose for several injections to blood, which is made possible by the long T_1 outside the blood.

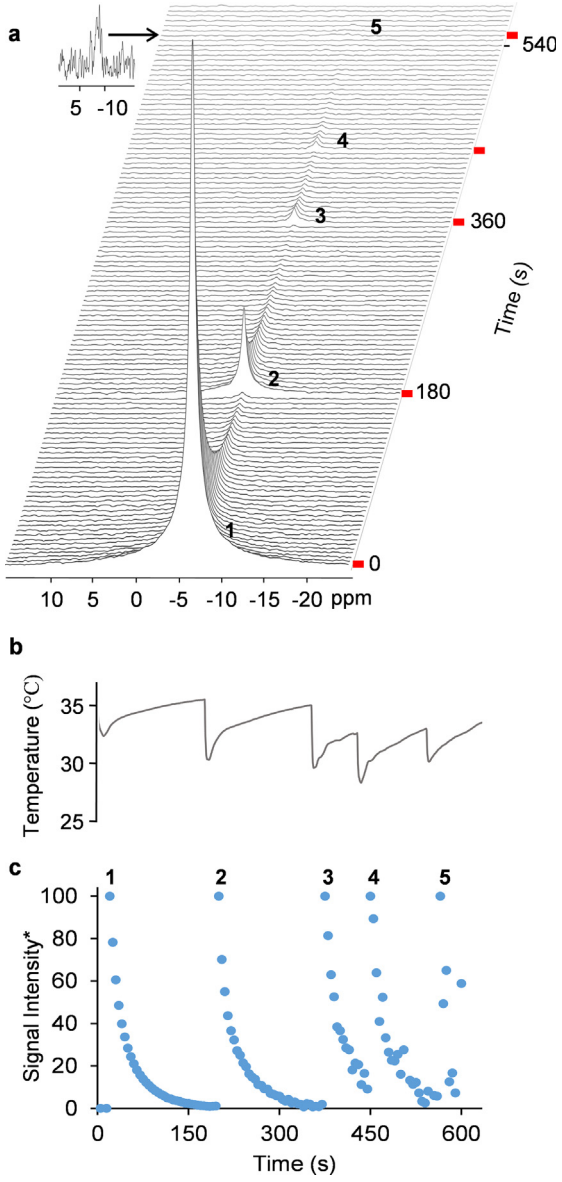

Fig. 4. Multiple hyperpolarized [^{15}N]nitrate injections to blood from a single hyperpolarized [^{15}N]nitrate dose. A solution of 32.6 mM hyperpolarized sodium [^{15}N]nitrate in saline was kept in an ice-water bath and *ca.* 1 mL volumes were injected to heparinized whole human blood in an NMR tube (4.5 mL). The injected volumes ranged in temperature from 16.4 to 1.7 °C. The corresponding temperature range in the blood sample was 36.4–28.4 °C. The red marks on the time axis show the injection times (0, 180, 360, 435, and 550 s). (a) ^{15}N spectra of the consecutively injected hyperpolarized [^{15}N]nitrate in whole blood. The spectra were acquired with a repetition time of 5 s and a flip angle of 10°. (b) An online temperature recording of the sample in the spectrometer. It can be seen that the injection of the hyperpolarized medium first lowers the temperature of the sample by up to 5 °C, and then the temperature stabilizes. (c) The signal intensities of the hyperpolarized site in the consecutive injections. *The intensities are shown normalized to the highest signal for each injection. The relative multiplication factors are 6 (decay 2), 39 (decay 3), 76 (decay 4) and 297 (decay 5). The T_1s in blood corresponding to the decays 1 and 2 were found to be 29 ± 2 s and 30 ± 3 s, respectively, the error represents the 95% confidence interval for the individual fits.

3. Discussion

We showed here that sodium [^{15}N]nitrate is a potential contrast agent for biomedical magnetic resonance applications in a hyperpolarized state. It is strictly water-soluble and its T_1 was found to be long (>100 s) compared to other water-soluble hyperpolarized sites. This long T_1 appeared insensitive to the water protonation

status or to salinity. However, as is the case for many compounds including water protons [44], its T_1 did decrease upon mixing with whole blood (T_1 of 29 ± 1 s, three measurements in two different blood samples, as described in Fig. 2e and in Fig. 4c – decay 1 and 2). Shortening of hyperpolarized sites T_1 in whole blood was previously shown by Harris et al. for [$^{15}N_2$]urea [38] and by Allouche-Arnon for [$^{13}C_1$]pyruvic acid [45].

Another important factor is the stability of this compound in whole blood and saliva. We could not detect any metabolism of nitrate to nitrite in the time frames investigated thus far (several minutes in blood and several hours in saliva). Therefore, these results suggest that the conversion to the reduced form is indeed low and that nitrate remains intact throughout the visualization window. In a much longer investigation of the order of several days to a month, we were able to detect conversion of [^{15}N]nitrate to [^{15}N]nitrite in two samples that contained human saliva (Supporting Information S2), showing that this conversion does occur, as expected, but that this conversion is likely far from detrimental to the safety of nitrate administration.

Nevertheless, the apparently favorable safety profile does not rely on the current NMR measurements but on previous direct investigation of nitrate injection to humans [27] which found the compound safe for injection for a dose that is very similar to the doses used in the current study. Converting the intravenous dose injected by Ellen et al. [27], which was found to be safe, to mL per min units we get 12.5 mL/min of a 0.15 M solution, which can be further converted to 6 mL/10 s of 50 mM solution. This is a routinely tolerable volume/time for human intravenous injection. A sodium nitrate solution of 50 mM is higher in concentration than the solution that was used here for consecutive injections to blood (32.6 mM). Suggesting that indeed such a safe dose of sodium [^{15}N] nitrate could be observed *in vivo*.

The non-metabolic nature of [^{15}N]nitrate is important in two ways: 1) in terms of safety, as nitrite is the bioactive product of nitrate, and 2) in terms of MR imaging. As for the latter, the non-metabolic nature makes this molecular probe suitable for perfusion or tissue retention imaging. Although many dDNP agents have been used in MR spectroscopic examinations– *i.e.* with the aim of demonstrating the hyperpolarized substrate metabolism– here we target another MR application in which such metabolism is not desired. First, because a bioactivity is not desired, and second because a single signal is easier to image without artifacts compared to simultaneous imaging of several signals, each with different chemical shifts (in the case of nitrate and nitrite – more than 230 ppm apart).

Another advantage of sodium [^{15}N]nitrate is that it is readily available from multiple suppliers and is a relatively inexpensive ^{15}N-labeled small molecule. Using holding in ice-cold temperatures, outside the blood, we were able to observe the hyperpolarized signal in blood for up to 9 min, using multiple injections, without any chemical modifications.

When comparing the T_1 of the [^{15}N]nitrate anion with the T_1 of the [^{15}N]nitrite anion, we note a significant difference. In the same solvent (D_2O), and in fact in the same sample, the T_1s of the [^{15}N] nitrate and the [^{15}N]nitrite were 100 s and 14 s, respectively. Nitric acid, HNO_3, is a strong acid, in contrast to nitrous acid, HNO_2, which is a weak acid, with a pKa of 3.15 [20]. This pKa difference may explain the T_1 difference: while the nitric acid is completely ionized in all solutions, the nitrous acid is in an equilibrium with the ionic form. At neutral pH, most of the nitrous acid is dissociated and the anion concentration is about 4 orders of magnitude higher than the concentration of the protonated nitrous acid. Therefore, the amount of nitrous acid expected in a sodium nitrite solution is very small. However, the quickly exchanging proton (or a deuteron) on the oxygen close to nitrogen, is likely to shorten the T_1 as has been previously observed for inorganic phosphate in acidic conditions [42].

We note that the polarization level achieved here for [^{15}N]nitrate, of 1%, although in line with previous studies [35,37,38,40], does suggest that this polarization could be improved. For ^{13}C sites, polarization levels of up to 37% were recorded in solution [31] and it appears reasonable that given optimization of the formulation for solid state polarization (glassing agents and radical) and physical conditions for DNP (magnetic field, temperature, and microwave irradiation), such an improvement in the polarization level may be attained for [^{15}N]nitrate as well. However, we note that commercial dDNP devices are currently not equipped with a solid-state polarization buildup monitoring capabilities for nuclei other than ^{13}C. This is a major limitation for such an optimization as these studies must be carried out by serial dissolutions, which are unfortunately costly and time consuming. Nevertheless, in the supporting information we describe such serial dissolutions designed for calculating the solid-state build-up time constant and then to optimize the microwave irradiation used for solid-state polarization (Supporting information S3 and S4, respectively).

The limitations of hyperpolarized nitrate imaging may include low sensitivity of ^{15}N compared to protons (sensitivity will decrease as the ratio of the gyromagnetic ratios to the third power) and high gradient power that will be required to achieved image resolution adequate for clinical imaging (gradient power is inversely proportional to the gyromagnetic constant of the nucleus). Despite these likely limitations, the promising nature of hyperpolarized [^{15}N]nitrate, the likely lack of background signal (leading to high contrast), and the need to develop new and safe contrast agents for MRI that leave no traces behind, warrants further research.

A possible limitation to the conclusions drawn from this study with regard to the ability to store the polarization of [^{15}N]nitrate for longer duration in cold temperatures is that we did not explore the influence of the magnetic field on the T_1 of [^{15}N]nitrate and the cold solution was maintained at the fringe field of the 5.8 T magnet (about 2 mT). Colell et al. [46] and Truong et al. [47] investigated the dependence of the T_1 of ^{15}N on the magnetic field for various substances. Colell et al. found for [^{15}N]α-cyano-4-hydroxycinnamic acid ([^{15}N]CHCA) and [^{15}N]nicotinamide that at a magnetic field larger than 1 T, the ^{15}N T_1s decreased at higher magnetic fields. For [^{15}N]CHCA, Colell et al. also reported that at magnetic fields lower than 1 T the ^{15}N T_1 increased with an increase in the magnetic field. However, Truong et al. found for [^{15}N]pyridine, that the ^{15}N T_1 decreased with a decrease in the magnetic field in the low magnetic field regime and possibly also in the high magnetic field regime (^{15}N $T_1^{9.4\ T} > {}^{15}$N $T_1^{6\ mT} > {}^{15}$N $T_1^{\mu T}$). Thus, the storage of the cold solution in the fringe field of the spectrometer was not necessarily advantageous for prolonging the T_1 of the hyperpolarized compound.

In summary, we show here a novel compound for studies of dDNP hyperpolarization that may become a useful agent for MRI. The likely MRI applications appear to be imaging of blood flow in blood vessels and human tissues either normal or pathological (perfusion) and possibly, due to its ionic nature, also demonstrate tissue retention- as it may linger in the extracellular space. The T_1 characteristics were shown to be favorable with regard to solvent protonation and salinity, and the stability in body fluids was observed by NMR, in agreement with a previous safety study for a similar dose. Further studies are warranted in order to 1) optimize the polarization process, and 2) visualize the hyperpolarized compound distribution in the body. For the latter, experiments in small animals are a necessary step. Unfortunately, our lab is presently not equipped to perform such a study and we hope that other labs in the field may capitalize on this knowledge.

4. Methods

4.1. Chemicals

Sodium [^{15}N]nitrate and sodium [^{15}N]nitrite were purchased from Sigma-Aldrich, Rehovot, Israel. The OXO63 radical (GE Healthcare, UK) was obtained from Oxford Instruments Molecular Biotools (Oxford, UK). [$^{15}N_2$]urea was purchased from Cambridge Isotope Laboratories (Andover, MA, USA).

4.2. Nitrate and nitrite formulations

To explore the hyperpolarized state of nitrate and the nitrite anions in solution the following formulations were prepared for solid-state polarization: for the nitrate anion, 85.2 mg of $Na^{15}NO_3$, 3.7 mg of OXO63 radical, 76 mg of glycerol, and 145 mg D_2O. For the nitrite anion, 59.5 mg of $Na^{15}NO_2$, 2.2 mg of OXO63 radical, and 129.65 mg of D_2O:[$^{13}C_3$]glycerol 7:3 mixture. Carbon-13 labeled glycerol was used to monitor the presence of the sample in the polarization chamber. For the samples that were not prepared with [$^{13}C_3$]glycerol, a small amount of [^{13}C,D_7]glucose (up to 13.3 mg) or [1-^{13}C]pyruvic acid (up to 1.8 mg) formulation was added as a dot on the cup wall – to indicate, using the polarizer ^{13}C spectrometer, that the sample is in the polarization chamber. A vitrification assay [48] showed that these formulations indeed formed a glass upon rapid freezing to cryogenic temperature (liquid nitrogen).

4.3. DNP spin polarization and dissolution

Spin polarization and fast dissolution were carried out in a dDNP set-up (HyperSense, Oxford Instruments Molecular Biotools, Oxford, UK). A microwave frequency of 94.100 GHz was determined as optimal (Supporting Information S4) and is in a general agreement with the findings of Reynolds et al. [49].

The dissolution process was performed as previously described [31] and detailed in the results section. Briefly: 20–90 mg of the sodium [^{15}N]nitrate formulation were placed in a polarization sample cup, polarized by microwave irradiation, and then quickly dissolved in 4 mL of superheated aqueous media (170 °C and 10 bar). Unless otherwise stated, the dissolved hyperpolarized solution was directly injected to a screw cup 10 mm NMR tube in a 5.8 T NMR spectrometer *via* a PTFE line of about 2.4 m length with 3 s of $He_{(g)}$ chase. This line was wrapped with a heating tape (MRC, Holon, Israel) that enabled control over the temperature of the dissolution medium arriving to the NMR tube directly or to a collection tube in the fringe field of the spectrometer. ^{15}N NMR spectra were continuously recorded immediately at the start of the dissolution process. The hyperpolarized signals appeared in the spectra at about 10–14 s from the start of the dissolution process (meaning that the dissolution process and the chase of the media into the NMR tube occurred within about 10–14 s). In the experiments in body fluids and in experiments in which the hyperpolarized solution was first cooled to temperatures below room temperature, the dissolution media was first collected in a conical tube placed in the spectrometer's fringe field, and then was injected by syringe *via* a PEEK line to the NMR tube that was placed in the magnet.

4.4. Modification of the hyperpolarized solution temperature prior to arrival to the spectrometer

The temperature of the solution leaving the dDNP device was not lower than 26 °C. For heating this hyperpolarized solution prior to arrival to the NMR tube, the PTFE line leading the hyperpolarized solution out of the spin polarization device was wrapped with a heating tape connected to a temperature controller (MRC, Holon, Israel). In this way, hyperpolarized solutions at temperatures higher than 26 °C could be obtained. For cooling the hyperpolarized solution, the heating tape was not turned on and the dissolution medium was mixed with 0 to 4 mL of D_2O at 2 °C in a collection tube placed in ice-water bath in the fringe field of the magnet, prior to injection.

4.5. ^{15}N NMR

^{15}N NMR spectroscopy was performed in a 5.8 T NMR spectrometer (RS2D, Mundolsheim, France), using a 10 mm broad-band NMR probe. The chemical shift scale of the spectra presented herein was calibrated based on a separate measurement of a [$^{15}N_2$]urea standard sample (4 M in H_2O:D_2O 80:20), carried out prior to hyperpolarized ^{15}N acquisitions, calibrating the [$^{15}N_2$]urea signal to −306 ppm (relative to nitromethane) [50–52]. For enhancement factor calculation, the spectra were collected with a high flip angle of 30° and a repetition time of 2 s. For T_1 calculation, the spectra were acquired with a low flip angle of 10° and a longer repetition time of 5–10 s.

4.6. Online temperature sensing in the NMR spectrometer

The temperature in the NMR tube was continuously monitored using an NMR compatible temperature probe (Osensa, Burnaby, BC, Canada). A typical example of such a measurement is shown in the Supporting Information S5.

4.7. Processing and data analysis

Spectral processing was performed using MNova (Mestrelab Research, Santiago de Compostela, Spain).

Determination of the T_1 of the hyperpolarized sites was performed by curve fitting of the signal decay to the following equation: $M(t) = M_o * e^{\left(\frac{-t}{T_1}\right)} * \cos\theta^{\left(\frac{t}{TR}\right)}$, in which TR, the time between excitations, and θ, the nutation angle of excitation, are known.

Curve fitting was performed using Matlab (Mathworks, Natick, MA, USA).

The absolute enhancement factor was determined by comparing the maximal SNR of the magnitude signal multiplied by the linewidth at half-height obtained under hyperpolarized conditions to the intensity of the thermal equilibrium signal of the same sample (analyzed in the same way). The spectrum at thermal equilibrium was acquired with the same nutation angle under fully relaxed conditions. The same spectral acquisition parameters (spectral width, number of points, receiver gain) and processing parameters (apodization, zero-filling) were used in the analysis of both spectra and the thermal equilibrium signal was corrected for the number of scans.

Acknowledgments

This project has received funding from the European Research Council (ERC) under grant agreement No. 338040 to R.K-B, from the European Union's Horizon 2020 research and innovation program under grant agreement No. 667192 and from the Israel Science Foundation under grant agreement number 1379/18.

Author contributions

AG, GS, JMG, and RKB conceived ideas. AG, SU, TH, AN-S and RKB designed the studies. AG, SU, and DS performed the experiments.

AG performed the analyses. RKB directly supervised the study. JS and JMG supported this study. All authors approved the final version of the manuscript.

Data availability

The data that support the findings of this study are available from the corresponding author on request.

Competing interests

The authors declare no competing financial interests.

Appendix A. Supplementary material

Supplementary data associated with this article can be found, in the online version, at https://doi.org/10.1016/j.jmr.2019.01.001.

References

[1] M.F. Tweedle, P. Wedeking, K. Kumar, Biodistribution of radiolabeled, formulated gadopentetate, gadoteridol, gadoterate, and gadodiamide in mice and rats, Invest. Radiol. 30 (6) (1995) 372–380.

[2] G.W. White, W.A. Gibby, M.F. Tweedle, Comparison of Gd(DTPA-BMA) (Omniscan) versus Gd(HP-DO3A) (ProHance) relative-to gadolinium retention in human bone tissue by inductively coupled plasma mass spectroscopy, Invest. Radiol. 41 (3) (2006) 272–278.

[3] T. Kanda, M. Osawa, H. Oba, K. Toyoda, J. Kotoku, T. Haruyama, K. Takeshita, S. Furui, High signal intensity in dentate nucleus on unenhanced T_1-weighted MR images: Association with linear versus macrocyclic gadolinium chelate administration, Radiology 275 (3) (2015) 803–809.

[4] Y. Errante, V. Cirimele, C.A. Mallio, V. Di Lazzaro, B.B. Zobel, C.C. Quattrocchi, Progressive increase of T_1 signal intensity of the dentate nucleus on unenhanced magnetic resonance images is associated with cumulative doses of intravenously administered gadodiamide in patients with normal renal function, suggesting dechelation, Investigat. Radiol. 49 (10) (2014) 685–690.

[5] E. Kanal, M.F. Tweedle, Residual or retained gadolinium: Practical implications for radiologists and our patients, Radiology 275 (3) (2015) 630–634.

[6] T. Kanda, K. Ishii, H. Kawaguchi, K. Kitajima, D. Takenaka, High signal intensity in the dentate nucleus and globus pallidus on unenhanced T_1-weighted MR images: Relationship with increasing cumulative dose of a gadolinium-based contrast material, Radiology 270 (3) (2014) 834–841.

[7] EMA EMA's final opinion confirms restrictions on use of linear gadolinium agents in body scans. http://www.ema.europa.eu/ema/index.jsp;curl=pages/medicines/pips/EMEA-001743-PIP01-14/pages/includes/document/pages/includes/document/pages/includes/document/index.jsp?curl=pages/medicines/human/referrals/Gadolinium-containing_contrast_agents/human_referral_prac_000056.jsp&mid=WC0b01ac05805c516f (Accessed December 2018).

[8] M. Birka, K.S. Wentker, E. Lusmoller, B. Arheilger, C.A. Wehe, M. Sperling, R. Stadler, U. Karst, Diagnosis of nephrogenic systemic fibrosis by means of elemental bioimaging and speciation analysis, Anal. Chem. 87 (6) (2015) 3321–3328.

[9] M.F. Tweedle, Gadolinium deposition: Is it chelated or dissociated gadolinium? How can we tell?, Magn Reson. Imaging 34 (10) (2016) 1377–1382.

[10] E. Kanal, Gadolinium based contrast agents (GBCA): Safety overview after 3 decades of clinical experience, Magn. Reson. Imaging 34 (10) (2016) 1341–1345.

[11] P. Marckmann, L. Skov, K. Rossen, A. Dupont, M.B. Damholt, J.G. Heaf, H.S. Thomsen, Nephrogenic systemic fibrosis: Suspected causative role of gadodiamide used for contrast-enhanced magnetic resonance imaging, J. Am. Soc. Nephrol. 17 (9) (2006) 2359–2362.

[12] H. Ersoy, F.J. Rybicki, Biochemical safety profiles of gadolinium-based extracellular contrast agents and nephrogenic systemic fibrosis, J. Magn. Reson. Imag. 26 (5) (2007) 1190–1197.

[13] J. Lohrke, A.L. Frisk, T. Frenzel, L. Schockel, M. Rosenbruch, G. Jost, D.C. Lenhard, M.A. Sieber, V. Nischwitz, A. Kuppers, H. Pietsch, Histology and gadolinium distribution in the rodent brain after the administration of cumulative high doses of linear and macrocyclic gadolinium-based contrast agents, Invest. Radiol. (2017).

[14] V. Gulani, F. Calamante, F.G. Shellock, E. Kanal, S.B. Reeder, Gadolinium deposition in the brain: summary of evidence and recommendations, The Lancet Neurology 16 (7) (2017) 564–570.

[15] D.L. Archer, Evidence that ingested nitrate and nitrite are beneficial to health, J. Food Prot. 65 (5) (2002) 872–875.

[16] E. Weitzberg, M. Hezel, J.O. Lundberg, Nitrate-nitrite-nitric oxide pathway implications for anesthesiology and intensive care, Anesthesiology 113 (6) (2010) 1460–1475.

[17] S. Shiva, Nitrite: A physiological store of nitric oxide and modulator of mitochondrial function, Redox Biol. 1 (1) (2013) 40–44.

[18] R.M. Pluta, E.H. Oldfield, K.D. Bakhtian, A.R. Fathi, R.K. Smith, H.L. DeVroom, M. Nahavandi, S. Woo, W.D. Figg, R.R. Lonser, Safety and feasibility of long-term intravenous sodium nitrite infusion in healthy volunteers, PLoS One 6 (1) (2011) 13.

[19] J.O. Lundberg, E. Weitzberg, Biology of nitrogen oxides in the gastrointestinal tract, Gut 62 (4) (2013) 616–629.

[20] A.R. Butler, M. Feelisch, Therapeutic uses of inorganic nitrite and nitrate - From the past to the future, Circulation 117 (16) (2008) 2151–2159.

[21] E.F. Sato, T. Choudhury, T. Nishikawa, M. Inoue, Dynamic aspect of reactive oxygen and nitric oxide in oral cavity, J. Clin. Biochem. Nutr. 42 (1) (2008) 8–13.

[22] A.C. Torregrossa, M. Aranke, N.S. Bryan, Nitric oxide and geriatrics: implications in diagnostics and treatment of the elderly, J. Geriatr. Cardiol. 8 (4) (2011) 230–242.

[23] E.A. Jansson, L. Huang, R. Malkey, M. Govoni, C. Nihlen, A. Olsson, M. Stensdotter, J. Petersson, L. Holm, E. Weitzberg, J.O. Lundberg, A mammalian functional nitrate reductase that regulates nitrite and nitric oxide homeostasis, Nat. Chem. Biol. 4 (7) (2008) 411–417.

[24] V. Kapil, A.B. Milsom, M. Okorie, S. Maleki-Toyserkani, F. Akram, F. Rehman, S. Arghandawi, V. Pearl, N. Benjamin, S. Loukogeorgakis, R. MacAllister, A.J. Hobbs, A.J. Webb, A. Ahluwalia, Inorganic nitrate supplementation lowers blood pressure in humans role for nitrite-derived NO, Hypertension 56 (2) (2010) 274–U174.

[25] M.R. Duranski, J.J.M. Greer, A. Dejam, S. Jaganmohan, N. Hogg, W. Langston, R.P. Patel, S.F. Yet, X.D. Wang, C.G. Kevil, M.T. Gladwin, D.J. Lefer, Cytoprotective effects of nitrite during in vivo ischemia-reperfusion of the heart and liver, J. Clin. Invest. 115 (5) (2005) 1232–1240.

[26] M. Gilchrist, A.C. Shore, N. Benjamin, Inorganic nitrate and nitrite and control of blood pressure, Cardiovasc. Res. 89 (3) (2011) 492–498.

[27] G. Ellen, P.L. Schuller, E. Bruijns, P. Froeling, H. Baadenhuijsen, Volatile N-nitrosamines, nitrate and nitrite in urine and saliva of healthy-volunteers after administration of large amounts of nitrate, IARC Sci. Publ. 41 (1982) 365–378.

[28] C. Damacena-Angelis, G.H. Oliveira-Paula, L.C. Pinheiro, E.J. Crevelin, R.L. Portella, L.A.B. Moraes, J.E. Tanus-Santos, Nitrate decreases xanthine oxidoreductase-mediated nitrite reductase activity and attenuates vascular and blood pressure responses to nitrite, Redox Biol. 12 (2017) 291–299.

[29] L.D. Roberts, T. Ashmore, A.O. Kotwica, S.A. Murfitt, B.O. Fernandez, M. Feelisch, A.J. Murray, J.L. Griffin, Inorganic nitrate promotes the browning of white adipose tissue through the nitrate-nitrite-nitric oxide pathway, Diabetes 64 (2) (2015) 471–484.

[30] B.L. Loudon, H. Noordali, N.D. Gollop, M.P. Frenneaux, M. Madhani, Present and future pharmacotherapeutic agents in heart failure: an evolving paradigm, Br. J. Pharmacol. 173 (12) (2016) 1911–1924.

[31] J.H. Ardenkjaer-Larsen, B. Fridlund, A. Gram, G. Hansson, L. Hansson, M.H. Lerche, R. Servin, M. Thaning, K. Golman, Increase in signal-to-noise ratio of > 10,000 times in liquid-state NMR, Proc. Natl. Acad. Sci. U. S. A. 100 (18) (2003) 10158–10163.

[32] N. Chattergoon, F. Martinez-Santiesteban, W.B. Handler, J.H. Ardenkjaer-Larsen, T.J. Scholl, Field dependence of T-1 for hyperpolarized 1-C-13 pyruvate, Contrast Media Mol. Imaging 8 (1) (2013) 57–62.

[33] M. Fuetterer, J. Busch, S.M. Peereboom, C. von Deuster, L. Wissmann, M. Lipiski, T. Fleischmann, N. Cesarovic, C.T. Stoeck, S. Kozerke, Hyperpolarized C-13 urea myocardial first-pass perfusion imaging using velocity-selective excitation, J. Cardiov. Magn. Reson. 19 (2017) 12.

[34] L.L. Lumata, M.E. Merritt, C.R. Malloy, A.D. Sherry, J. van Tol, L.K. Song, Z. Kovacs, Dissolution DNP-NMR spectroscopy using galvinoxyl as a polarizing agent, J. Magn. Reson. 227 (2013) 14–19.

[35] K. Kumagai, K. Kawashima, M. Akakabe, M. Tsuda, T. Abe, M. Tsuda, Synthesis and hyperpolarized N-15 NMR studies of N-15-choline-d(13), Tetrahedron 69 (19) (2013) 3896–3900.

[36] H. Nonaka, M. Hirano, Y. Imakura, Y. Takakusagi, K. Ichikawa, S. Sando, Design of a N-15 molecular unit to achieve long retention of hyperpolarized spin state, Sci. Rep. 7 (2017) 6.

[37] E. Chiavazza, A. Viale, M. Karlsson, S. Aime, N-15-Permethylated amino acids as efficient probes for MRI-DNP applications, Contrast Media Mol. Imaging 8 (5) (2013) 417–421.

[38] T. Harris, A. Gamliel, S. Uppala, A. Nardi-Schreiber, J. Sosna, J.M. Gomori, R. Katz-Brull, Long-lived 15N hyperpolarization and rapid relaxation as a potential basis for repeated first pass perfusion imaging - marked effects of deuteration and temperature, ChemPhysChem 19 (2018) 2148–2152.

[39] A.W. Barb, S.K. Hekmatyar, J.N. Glushka, J.H. Prestegard, Exchange facilitated indirect detection of hyperpolarized (ND2)-N-15-amido-glutamine, J. Magn. Reson. 212 (2) (2011) 304–310.

[40] C. Gabellieri, S. Reynolds, A. Lavie, G.S. Payne, M.O. Leach, T.R. Eykyn, Therapeutic target metabolism observed using hyperpolarized N-15 choline, J. Am. Chem. Soc. 130 (14) (2008) 4598-+.

[41] T. Saluvere, E. Lippmaa, Spin-lattice relaxation of N-15 nuclei, Chem. Phys. Lett. 7 (5) (1970) 545–548.

[42] A. Nardi-Schreiber, A. Gamliel, T. Harris, G. Sapir, J. Sosna, J.M. Gomori, R. Katz-Brull, Biochemical phosphates observed using hyperpolarized P-31 in physiological aqueous solutions, Nat. Commun. 8 (2017) 7.

[43] H. Allouche-Arnon, T. Wade, L.F. Waldner, V.N. Miller, J.M. Gomori, R. Katz-Brull, C.A. McKenzie, In vivo magnetic resonance imaging of glucose - initial experience, Contrast Media Mol. Imaging 8 (1) (2013) 72–82.

[44] J.M. Gomori, R.I. Grossman, C. Yu-Ip, T. Asakura, NMR relaxation times of blood: dependence on field strength, oxidation state, and cell integrity, J. Comput. Assist. Tomogr. 11 (4) (1987) 684–690.
[45] H. Allouche-Arnon, M.H. Lerche, M. Karlsson, R.E. Lenkinski, R. Katz-Brull, Deuteration of a molecular probe for DNP hyperpolarization–a new approach and validation for choline chloride, Contrast Media Mol. Imaging 6 (6) (2011) 499.
[46] J.F.P. Colell, M. Emondts, A.W.J. Logan, K. Shen, J. Bae, R.V. Shchepin, G.X. Ortiz, P. Spannring, Q. Wang, S.J. Malcolmson, E.Y. Chekmenev, M.C. Feiters, F. Rutjes, B. Blumich, T. Theis, W.S. Warren, Direct hyperpolarization of nitrogen-15 in aqueous media with parahydrogen in reversible exchange, J. Am. Chem. Soc. 139 (23) (2017) 7761–7767.
[47] M.L. Truong, T. Theis, A.M. Coffey, R.V. Shchepin, K.W. Waddell, F. Shi, B.M. Goodson, W.S. Warren, E.Y. Chekmenev, ^{15}N hyperpolarization by reversible exchange using SABRE-SHEATH, J. Phys. Chem. C 119 (16) (2015) 8786–8797.
[48] M. Karlsson, P.R. Jensen, J.O. Duus, S. Meier, M.H. Lerche, Development of dissolution DNP-MR substrates for metabolic research, Appl. Magn. Reson. 43 (1–2) (2012) 223–236.
[49] S. Reynolds, H. Patel, Monitoring the solid-state polarization of C-13, N-15, H-2, Si-29 and P-31, Appl. Magn. Reson. 34 (3–4) (2008) 495–508.
[50] R.K. Harris, E.D. Becker, S.M.C. De Menezes, R. Goodfellow, P. Granger, NMR nomenclature. Nuclear spin properties and conventions for chemical shifts - (IUPAC recommendations 2001), Pure Appl. Chem. 73 (11) (2001) 1795–1818.
[51] A. Geissler, K. Kanamori, B.D. Ross, Real-time study of the urea cycle using N-15 NMR in the isolated perfused-rat-liver, Biochem. J. 287 (1992) 813–820.
[52] P.R. Srinivasan, R.L. Lichter, N-15 nuclear magnetic-resonance spectroscopy - evaluation of chemical-shift references, J. Magn. Reson. 28 (2) (1977) 227–234.